

# Structural Behavior of FRP Composite Bridge Deck Panels

P. Alagusundaramoorthy<sup>1</sup>; I. E. Harik, M.ASCE<sup>2</sup>; and C. C. Choo<sup>3</sup>

**Abstract:** Fiber-reinforced polymer (FRP) composite bridge deck panels are high-strength, corrosion resistant, weather resistant, etc., making them attractive for use in new construction or retrofit of existing bridges. This study evaluated the force-deformation responses of FRP composite bridge deck panels under AASHTO MS 22.5 (HS25) truck wheel load and up to failure. Tests were conducted on 16 FRP composite deck panels and four reinforced concrete conventional deck panels. The test results of FRP composite deck panels were compared with the flexural, shear, and deflection performance criteria per Ohio Department of Transportation specifications, and with the test results of reinforced concrete deck panels. The flexural and shear rigidities of FRP composite deck panels were calculated. The response of all panels under service load, factored load, cyclic loading, and the mode of failure were reported. The tested bridge deck panels satisfied the performance criteria. The safety factor against failure varies from 3 to 8.

**DOI:** 10.1061/(ASCE)1084-0702(2006)11:4(384)

**CE Database subject headings:** Bridge decks; Fiber reinforced polymers; Static tests; Cyclic tests; Failure modes; Safety factors; Structural behavior; Composite structures.

## Introduction

The deterioration of structures in aggressive environments such as marine structures, bridges subjected to deicing salts, industrial buildings, and water and wastewater treatment facilities, caused by the corrosion of steel is a significant problem that would eventually lead to loss of serviceability. Techniques, such as epoxy coated steel bars and cathodic protection, have been used to inhibit corrosion, but their long-term reliability is still being questioned. Rapid deterioration of bridge structures and the heavy expenditures involved in their repair and replacements are matters of serious concern. Just as the causes of bridge deterioration are complex and numerous, so are the solutions to the problem. One such solution is the use of alternative reinforcement to better resist corrosion. The superior characteristics of composite materials such as strength, corrosion and weather resistance, long term durability, etc., make fiber-reinforced polymer (FRP) attractive for use in new construction or retrofit of existing ones. The design of FRP bridge deck system is stiffness driven and an accurate evaluation of load deflection response is required.

Alampalli et al. (2002) presented the design, fabrication, and installation procedures, and proof testing of FRP composite bridge deck panels for a short span bridge. Lopez-Anido and Xu (2002) conducted analytical and experimental studies on half-scale hybrid FRP glulam panels and presented the structural

characteristics of these panels. Aref and Parsons (2000) outlined the steps involved in the design of a modular FRP bridge. Bakht et al. (2000) presented the design procedures of FRP structures in the Canadian Bridge Design Code Provisions for fiber-reinforced structures. Burgueno et al. (2001) studied the behavior of FRP composite bridge superstructure conducting experimental and analytical studies. Dutta et al. (2003) performed fatigue tests on FRP deck panels and studied their behavior under extreme weather conditions. Davalos et al. (2001) presented an analytical procedure for FRP honeycomb sandwich panels based on analytical and experimental studies. Foster et al. (2000) demonstrated the installation and field testing of the FRP composite highway bridge. Gan et al. (1999) reported the global and local stiffness, maximum stresses and buckling strength of various section profiles of pultruded deck panels. Harik et al. (1999) determined the factor of safety against failure of hybrid FRP/concrete composite bridge deck panels based on experimental studies. Hayes et al. (2000) and Kumar et al. (2004) developed and studied FRP composite bridge decks by assembling the pultruded components. Static and fatigue tests were conducted on models of hybrid FRP/concrete composite bridge structures (Kitane et al. 2004) and on models of composite bridge decks (Youn and Chang 1998).

The objectives of this study are: (1) to evaluate the static load-deflection response of FRP composite bridge deck panels, fabricated using four different manufacturing processes; (2) to compare the test results with the performance criteria (i.e., flexure, shear, and deflection) per the Ohio Department of Transportation (ODOT) specifications, and with the test results of reinforced concrete bridge deck panels; and (3) to calculate the flexural and shear rigidities ( $EI$  and  $GA_w$ ) of the panels. To achieve these objectives, the following tasks were carried out: (1) static testing of FRP bridge deck panels under the design wheel load of 116 kN (26 kip) [89 kN (20 kip) wheel load+30% for impact] for the American Association of State Highways and Transportation Officials (AASHTO) Standard MS 22.5 (HS25) truck wheel load (AASHTO 2002); (2) cyclic loading of bridge deck panels under the service load of 53.4 kN (12 kip) (4 kip/ft width) with load cycle from 0 to 53.4 kN (12 kip) and

<sup>1</sup>Assistant Professor, Composites Technology Centre, IIT Madras, India 600 036. E-mail: aspara0@iitm.ac.in

<sup>2</sup>Professor, Dept. of Civil Engineering, Univ. of Kentucky, Lexington, KY 40506 (corresponding author). E-mail: iharik@engr.uky.edu

<sup>3</sup>Research Professor, Kentucky Transportation Center, Univ. of Kentucky, Lexington, KY 40506.

Note. Discussion open until December 1, 2006. Separate discussions must be submitted for individual papers. To extend the closing date by one month, a written request must be filed with the ASCE Managing Editor. The manuscript for this paper was submitted for review and possible publication on May 27, 2005; approved on September 21, 2005. This paper is part of the *Journal of Bridge Engineering*, Vol. 11, No. 4, July 1, 2006. ©ASCE, ISSN 1084-0702/2006/4-384-393/\$25.00.

back to zero, and repeat the cycle five times, and design wheel load of 116 kN (26 kip) with load cycle from 0 to 116 kN (26 kip) and back to zero, and repeat the cycle five times; (3) loading to failure; (4) comparison of deflections of FRP deck panels with the deflection criteria specified by ODOT, and the reinforced concrete deck panels; (5) comparison of strains and ultimate load of FRP deck panels with the flexure criteria specified by ODOT; (6) comparison of shear capacity of the deck panels with the shear criteria specified by ODOT; (7) evaluation of the failure modes; (8) calculation of flexural rigidities ( $EI$ ) and shear rigidities ( $GA_w$ ); and (9) determination of the safety factor against failure. The results were used to model the First Salem Bridge, Ohio.

## Test Specimens

The behavior of FRP composite bridge deck panels under service load, design wheel load, and failure load was examined by testing twelve single span and four double span FRP composite bridge deck panels along with four reinforced concrete (RC) control/baseline panels at the University of Kentucky Structural Engineering Laboratory. The FRP bridge deck panels were fabricated and supplied by four different manufacturers. Each manufacturer supplied one set of panels consisting of three single span and one double span bridge deck panels. The total length, effective length (distance between centerlines of supports), width, and average thickness of all single and double span deck panels are shown in Table 1.

The baseline/control panels were reinforced concrete deck panels [Fig. 1(a)]. The single span deck panels were designated as RC1, RC2, and RC3, and the double span deck panel was RC4. The pultruded FRP deck panels supplied by Creative Pultrusions (CP) consisted of double trapezoid and hexagonal pultruded components that were bonded and interlocked to form the deck panel [Fig. 1(b)]. The single span deck panels were designated as CP1, CP2, and CP3, and the double span deck panel was CP4. The hybrid FRP/concrete deck panels supplied by Composite Deck Solutions (CDS) were fabricated using concrete reinforced with glass fiber reinforced polymer (GFRP) rebars, and cast over pultruded GFRP tubular sections [Fig. 1(c)]. The pultruded tubular section acts as the stay-in-place form and bottom reinforcing mat in a concrete deck with a top reinforcing mat made up of GFRP rebars. The single span deck panels were designated as CDS1, CDS2, and CDS3, and the double span deck panel was CDS4. The Seaman composite resin infusion molding process (SCRIMP) FRP composite fiberglass deck panels supplied by Hardcore Composites (HC) were fabricated using the "cell core" technology in conjunction with SCRIMP. The cell core is foam wrapped with fiberglass fabric to create an internal lattice structure. The composite deck comprised of multiple wrapped cells with upper and lower fiberglass fabric skin faces [Fig. 1(d)]. The multiple wrapped cells form the longitudinal and transverse stiffening webs to create a deck with bidirectional stiffness. The single span deck panels were designated as HC1, HC2, and HC3, and the double span deck panel was HC4. The contact molding hand layup FRP fiberglass deck panels supplied by Infrastructure Composites International (ICI) consisted of core craft corrugated core sandwich system. The basic system is a single-tier sandwich panel with a standard core configuration [Fig. 1(e)]. The flats of the core would be in the direction normal to traffic flow. The single span deck panels were designated as ICI1, ICI2, and ICI3, and the double span deck panel was ICI4.

**Table 1.** Dimensions of Bridge Deck Panels

Details (mm)	Bridge deck panels																			
	Reinforced concrete				Creative pultrusions				Composite deck solutions				Hardcore composites				Infrastructure Composites International			
	RC1	RC2	RC3	RC4 <sup>a</sup>	CP1	CP2	CP3	CP4 <sup>a</sup>	CDS1	CDS2	CDS3	CDS4 <sup>a</sup>	HC1	HC2	HC3	HC4 <sup>a</sup>	ICI1	ICI2	ICI3	ICI4 <sup>a</sup>
Total length	2,743	3,353	3,962	5,791 <sup>b</sup>	2,743	3,353	3,962	5,791 <sup>b</sup>	2,743	3,353	3,962	6,096 <sup>b</sup>	2,743	3,353	3,962	6,096 <sup>b</sup>	2,743	3,353	3,962	6,096 <sup>b</sup>
Effective length <sup>c</sup>	2,438	3,048	3,658	2,743 <sup>d</sup>	2,438	3,048	3,658	2,743 <sup>d</sup>	2,438	3,048	3,658	2,743 <sup>d</sup>	2,438	3,048	3,658	2,743 <sup>d</sup>	2,438	3,048	3,658	2,743 <sup>d</sup>
Width	914	914	914	1,067	914	914	914	914	914	914	914	914	914	914	914	914	914	914	914	914
Thickness <sup>e</sup>	188	203	224	185	203	203	203	203	203	241	254	203	216	229	241	203	211	241	249	203

<sup>a</sup>Double span panel.

<sup>b</sup>Total length of the double span panel.

<sup>c</sup>Distance between centerlines of supports.

<sup>d</sup>Effective length in each span of the double span panel.

<sup>e</sup>Average thickness (1 in. = 25.4 mm).

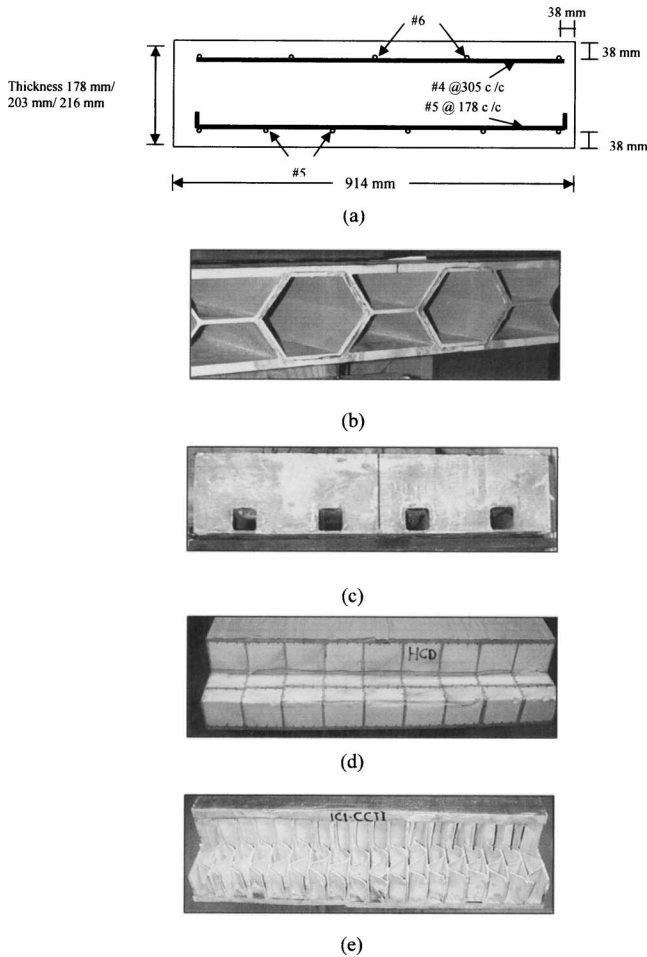


**Fig. 1.** Cross sections of bridge deck panels: (a) reinforced concrete; (b) creative pultrusions; (c) composite deck solutions; (d) hardcore composites; (e) Infrastructure Composites International

## Test Procedure

A test rig capable of applying a maximum load of 3,586 kN (800,000 lb) and testing of single and double span panels up to a maximum length of 13.7 m (45 ft) and breadth of 1.5 m (5 ft), was specially designed and fabricated. Hydraulic jacks of 150 mm (5.9 in.) stroke and a capacity of 1,800 kN (400,000 lb) were used for testing. Three point bending tests were performed on these panels. The load was transmitted through a rectangular plate of size 559 mm×229 mm×50 mm (22 in.×9 in.×2 in.) to the deck panel to represent the AASHTO MS 22.5 (HS25) standard truck wheel load. A rubber pad having the same dimensions as the steel plate with a thickness of 13 mm (0.5 in.) was placed between the deck panel and the steel plate in order to minimize the abrasion between the steel plate and the deck panel, and to simulate the rubber tire imprint. The top of the ram was provided with a spherical cap so that if any tilting of the plate were to occur during loading, the spherical cap would adjust in such a way that only a perpendicular load was applied to the deck panel. The details of the test setup, typical for double span deck panels, are shown in Fig. 2(a).

Disposable electrical resistance strain gauges of 6.35 mm (0.25 in.) long were mounted on the midsection of the panels. Reusable strain gauges of 76.2 mm (3 in.) long were attached to the concrete side of CDS and RC deck panels to measure the

tensile and compressive strains. Vertical deflections at three points along the midsection and at quarter span from both supports were measured using linear variable deflection transducers (LVDTs). The location of various strain gauges on double span panels are shown in Fig. 2(b), and the location of LVDTs are shown in Fig. 2(c). All strain gauges, LVDTs, and load cell were connected to a computer data acquisition system.

## Load Steps

The deck panels were initially loaded gradually up to 9 kN (2,000 lb) and then released. This operation was repeated twice to ensure the loading edges (rubber pad) remained in proper contact with the specimen. The deck panels were then loaded according to the following sequence:

1. Load Step (1): Load cycle from 0 to 116 kN (26 kip) and back to zero in order to establish a baseline curve;
2. Load Step (2): load cycle from 0 to 53.4 kN (12 kip) and back to zero, and repeat the cycle five times to study the response under service load;
3. Load Step (3): load cycle from 0 to 116 kN (26 kip) and back to zero, and repeat the cycle five times to study the response under design wheel load; and
4. Load Step (4): loading from zero to failure.

The deck panels were loaded at the rate of 10 kN/min (2,248 lb/min), and the data were continuously recorded at 5 s intervals.

## Performance Criteria

The ODOT specified the performance criteria for flexure, shear, and deflection for the FRP bridge deck panels. The deflection limits for FRP deck panels are based on the deflection calculations/limits for conventional reinforced concrete deck panels (Table 2), and they varied from  $L/596$  to  $L/762$  for single spans, and  $L/851$  to  $L/1,097$  for continuous span bridge deck panels, respectively. The deck panels in the First Salem Bridge will be continuous. Consequently, the deflection limit of  $L/800$  is satisfied.

The flexure criteria is based on the following: (1) the maximum allowable strain is limited to 20% of the ultimate strain under service load of  $LL+IL+DL$ , in which  $LL$ =live load,  $IL$ =impact load, and  $DL$ =dead load; (2) the maximum allowable dead load strain is limited to 10% of the ultimate strain [this includes 2.9 kPa (60 psf) of future wearing surface]; (3) the maximum factored load of  $1.3[1.67(LL+IL)+DL]<50%$  of ultimate load capacity of FRP deck panels; and (4) the maximum factored load of  $1.3[1.67(LL+IL)+DL]<100%$  of ultimate load capacity for hybrid FRP/concrete deck panels.

The shear criteria is based on the following: (1) the shear capacity shall be equal or greater than that of a corresponding RC conventional deck panel [the shear capacity of the deck is 146 kN/m (10,000 lb/ft) of width]; (2) the maximum allowable shear at a factored load of  $1.3[1.67(LL+IL)+DL]$  shall be  $<45%$  of the ultimate shear load capacity for all nonhybrid FRP deck panels; and (3) the maximum allowable shear for a factored load of  $1.3[1.67(LL+IL)+DL]$  shall be  $<100%$  of the ultimate shear capacity for hybrid FRP/concrete deck panels.

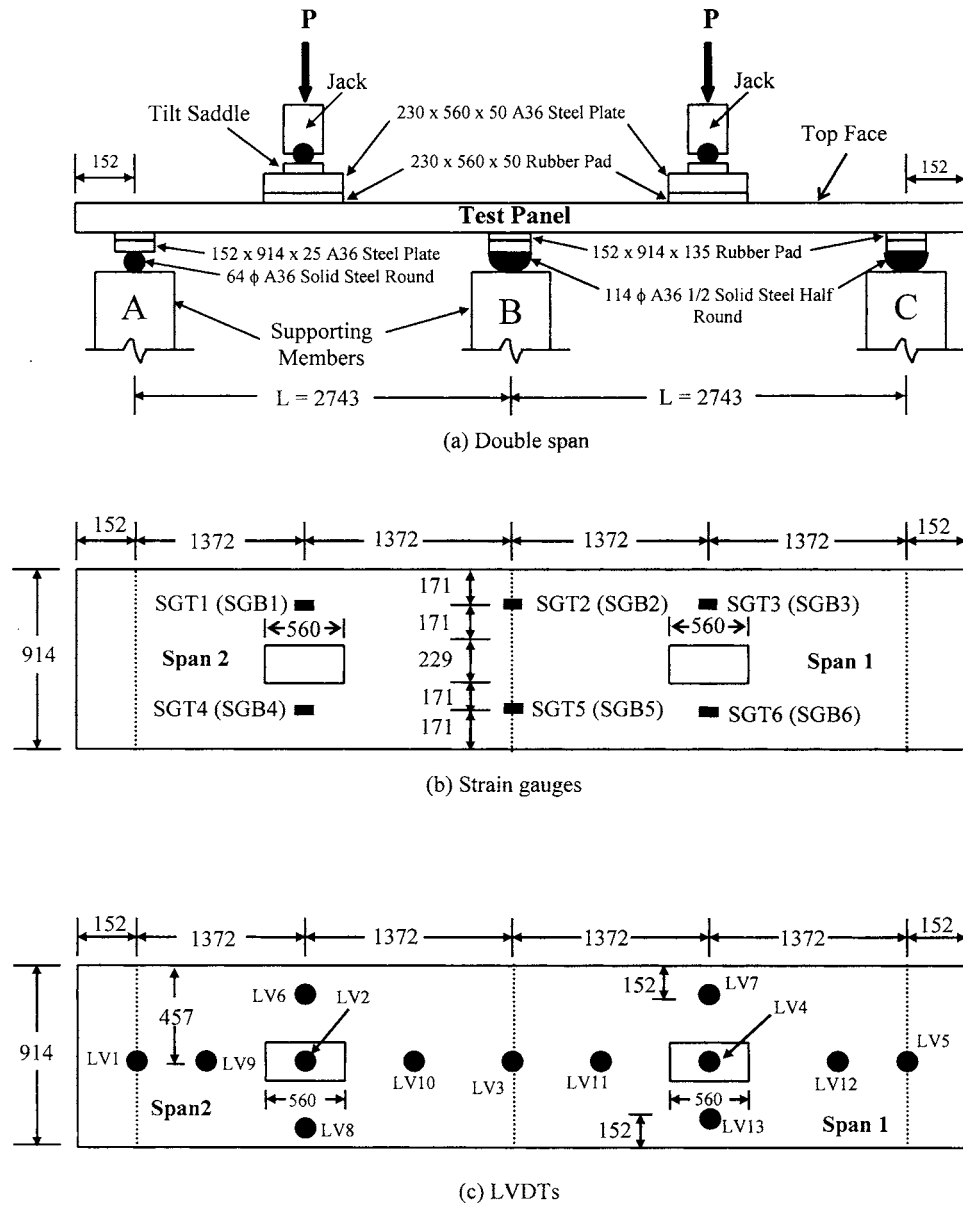


Fig. 2. Test setup for double span deck panel (note: units are in millimeters)

Table 2. Deflection Limits for FRP Deck Panels Specified by Ohio Department of Transportation

Span $L^a$ (mm)	Clear span used for design (mm)	Deck thickness <sup>b</sup> (mm)	Applied service load <sup>c</sup> (kN)	Single span deflection <sup>d,e</sup>		Continuous span deflection <sup>e</sup>	
				$(L/k)^f$	(mm)	$(L/k)^f$	(mm)
2,438	2,286	203	53.4	$L/762$	3.2	$L/975$	2.5
2,743	2,591	203	53.4	$L/596$	4.6	$L/1,097$	2.5
3,048	2,896	229	53.4	$L/709$	4.3	$L/1,089$	2.8
3,658	3,505	241	53.4	$L/600$	6.1	$L/851$	4.3

<sup>a</sup>Measured distance between centerline of the supports.

<sup>b</sup>Manufacturers are permitted to increase the depth of their decks within +12.7 mm of the thickness shown for the 3,048 and 3,658 mm span lengths.

<sup>c</sup>Load is to be applied over 229 mm × 559 mm contact area.

<sup>d</sup>Simple span values are to be used during testing to evaluate the FRP decks relative to an RC deck [1 in. = 25.4 mm (1 kip = 4.4482 kN)].

<sup>e</sup>The deck panels in the First Salem Bridge will be continuous.

<sup>f</sup> $L/k$  = deflection limit designation;  $L$  = span length as indicated in <sup>a</sup>; and  $k$  = deflection coefficient.

## Flexural and Shear Rigidities

The flexural and shear rigidities ( $EI$  and  $GA_w$ , respectively) of FRP deck panels were calculated by: (1) conducting a linear regression analysis on the load/deflection response of the baseline curves using the first-order shear deformation beam equations; (2) using first order beam equations without considering the shear deformation; and (3) using the moment–curvature relationship on the load/strain response of the baseline curves.

The first-order shear deformation beam equations (shown below) were used to calculate the flexural and shear rigidities in single span panels

$$\delta_{1/2} = \frac{PL^3}{48EI} + \frac{PL}{4GA_w} \quad (1)$$

$$\delta_{1/4} = \frac{11PL^3}{768EI} + \frac{PL}{8GA_w} \quad (2)$$

in which  $\delta_{1/2}$ =deflection at a distance of  $L/2$  from Support A;  $\delta_{1/4}$ =deflection at a distance of  $L/4$  from Support A;  $P$ =patch load distributed over a region of 229 mm×559 mm (9 in.×22 in.) at the center of the panel; and  $L$ =effective span length.

The values of  $\delta_{1/4}$  and  $\delta_{1/2}$  for a particular load ( $P$ ) can be obtained from the experimental load/deflection curves and substituted in Eqs. (1) and (2) and Eqs. (1) and (2) will have two unknowns ( $EI$  and  $GA_w$ ) and are found by solving these two equations. The first-order shear deformation beam equations (shown below) were used to calculate the flexural and shear rigidities in double span panels following the same procedures

$$\delta_{1/2} = \frac{7PL^3}{768EI} + \frac{5PL}{32GA_w} \quad (3)$$

$$\delta_{1/4} = \frac{43PL^3}{6144EI} + \frac{5PL}{64GA_w} \quad (4)$$

The first order beam equations (shown below) for single and double span panels without considering the shear deformations were also used to calculate the flexural rigidity ( $EI$ ) from the load/deflection response of the baseline curves

$$\delta_{1/2} = \frac{PL^3}{48EI} \quad (5)$$

$$\delta_{1/2} = \frac{7PL^3}{768EI} \quad (6)$$

The moment–curvature relationship shown in the following equation was used to calculate the flexural rigidity ( $EI$ ) using the load/strain response of the baseline curves

$$\frac{M}{I} = \frac{\sigma}{y} = \frac{E}{R} \quad (7)$$

in which  $M$ =bending moment;  $I$ =moment of inertia;  $\sigma$ =bending stress;  $y$ =distance of outermost fiber from neutral axis;  $E$ =Young's modulus; and  $R$ =radius of curvature.

The neutral axis can be located using the strains ( $\epsilon$ ) on the top and bottom faces of the panel and the value of  $EI$  is calculated using the following equation:

$$EI = \frac{My}{\epsilon} \quad (8)$$

## Results and Discussions

The measured deflection at the applied service load of 53.4 kN (12 kip), baseline deflection, and allowable deflections are presented in Table 3. The measured strain under service load of (LL+IL+DL) and DL, and allowable strain are also presented in Table 3. The ultimate load (failure load), required load specified by ODOT, maximum deflection at ultimate load (failure load), and mode of failure are presented in Table 4. The load at failure and maximum deflection at failure were also compared with their respective baseline failure load and maximum deflection (Table 4). The safety factor against failure of all tested FRP bridge deck panels was calculated as failure load/factored load, shown in Table 4. The calculated values of flexural and shear rigidities for the single and double span deck panels are presented in Tables 5 and 6, respectively. The following sections discuss the results for the different deck panels.

### RC Bridge Deck Panels

The load/deflection relations [Load Steps (2) and (3)] showed that the stiffness of the decks RC1, RC2, RC3, and RC4 remained constant during cyclic loading. Flexural cracks were formed initially in the concrete tension zone in single span panels RC1, RC2, and RC3, and then throughout the length of the panel. As the load was further increased, the flexural crack width and depth increased, and specimens RC1, RC2, and RC3 failed in flexure. Flexural cracks were formed initially in the concrete tension zone in Span 1 and Span 2 of double span panel RC4, and then throughout the length of the panel. The flexural crack width and depth increased, and shear cracks initiated on further increase in load. The specimen RC4 failed due to flexure-shear near the middle support. The specimens RC1, RC2, RC3, and RC4 started load shedding immediately after the failure load was reached, and failure was observed to be sudden. Crushing of concrete at the loading point was observed in all RC deck panels after failure.

### Pultruded FRP Bridge Deck Panels

The load/deflection relations [Load Steps (2) and (3)] showed that the stiffness of the decks CP1, CP2, CP3, and CP4 remained constant during cyclic loading. Cracking sound due to debonding of the joints of the pultruded sections was observed at a load of 287 kN (64,000 lb) in CP1, 269 kN (60,000 lb) in CP2, 211 kN (47,000 lb) in CP3, and 179 kN (40,000 lb) in CP4. All pultruded FRP deck panels experienced load shedding immediately after the failure load was reached, and failed suddenly. Buckling of the web was observed at the loading point in all panels, when viewed through the end sections after failure. Upon unloading deck panels CP1 and CP4 returned to their original shape, and the top and bottom surfaces looked almost like the original untested specimen. Deck panels CP2 and CP3, however, did not return to

**Table 3.** Comparison of Deflections and Strains of FRP Deck Panels with the Deflection Criteria and Flexure Criteria

Specimen	Centerline deflection at applied service load of 53.4 kN			Maximum strain at LL+IL+DL		Maximum strain at DL	
	Measured <sup>a</sup> (mm)	Baseline <sup>b</sup> (mm)	Allowable <sup>c</sup> (mm)	Measured <sup>d</sup> ( $\mu\epsilon$ )	Allowable <sup>e</sup> ( $\mu\epsilon$ )	Measured <sup>d</sup> ( $\mu\epsilon$ )	Allowable <sup>e</sup> ( $\mu\epsilon$ )
CP1	2.3	3.6	3.2	808	3,200	80	1,600
CP2	4.1	5.0	4.3	969	3,200	71	1,600
CP3	6.1	6.7	6.1	1,399	3,200	125	1,600
CP4 Span 1 <sup>f</sup>	2.2	1.4	4.6	660 <sup>g</sup>	3,200	92 <sup>g</sup>	1,600
CP4 Span 2 <sup>f</sup>	2.6	1.5	4.6	660 <sup>g</sup>	3,200	92 <sup>g</sup>	1,600
CDS1	1.0	3.6	3.2	659	3,400	42	1,700
CDS2	1.3	5.0	4.3	727	3,400	117	1,700
CDS3	2.5	6.7	6.1	1,027	3,400	202	1,700
CDS4 Span 1 <sup>f</sup>	1.3	1.4	4.6	827 <sup>g</sup>	3,400	193 <sup>g</sup>	1,700
CDS4 Span 2 <sup>f</sup>	1.3	1.5	4.6	827 <sup>g</sup>	3,400	193 <sup>g</sup>	1,700
HC1	3.4	3.6	3.2	1,230	4,100	91	2,050
HC2	4.6	5.0	4.3	1,188	4,100	102	2,050
HC3	6.3	6.7	6.1	1,400	4,100	156	2,050
HC4 Span 1 <sup>f</sup>	2.5	1.4	4.6	1,205 <sup>g</sup>	4,100	176 <sup>g</sup>	2,050
HC4 Span 2 <sup>f</sup>	2.6	1.5	4.6	1,205 <sup>g</sup>	4,100	176 <sup>g</sup>	2,050
ICI1	2.3	3.6	3.2	974	4,200	69	2,100
ICI2	3.3	5.0	4.3	1,011	4,200	94	2,100
ICI3	4.4	6.7	6.1	1,118	4,200	118	2,100
ICI4 Span 1 <sup>f</sup>	1.9 <sup>f</sup>	1.4	4.6	932 <sup>g</sup>	4,200	130 <sup>g</sup>	2,100
ICI4 Span 2 <sup>f</sup>	1.9 <sup>f</sup>	1.5	4.6	932 <sup>g</sup>	4,200	130 <sup>g</sup>	2,100

<sup>a</sup>The centerline deflections are derived by interpolation from the baseline deflection curves.

<sup>b</sup>The baseline deflection is obtained from tests conducted on conventional RC deck panels.

<sup>c</sup>The allowable deflections are provided by the Ohio Department of Transportation.

<sup>d</sup>The centerline strains are derived by interpolation from the baseline strain curves.

<sup>e</sup>The allowable strain=20% of maximum strain of the FRP coupon test.

<sup>f</sup>Span 1 and Span 2 for the two span panel are shown in Fig. 2.

<sup>g</sup>The maximum strain is measured along the middle support in the double span panel [1 in.=25.4 mm (1 kip=4.4482 kN)].

their original shape. Debonding of joints at the end sections of panels CP2 and CP3 was observed after failure. Failure of the pultruded FRP deck panels was due to the debonding of the pultruded components surrounding the loaded region and punching at the loading point [Fig. 3(a)]. The safety factor against failure varied from 5.6 to 5.7.

### Hybrid FRP/Concrete Bridge Deck Panels

The load/deflection relations [Load Steps (2) and (3)] showed that the stiffness of decks CDS1, CDS2, CDS3, and CDS4 remained constant during cyclic loading. Flexural cracks formed initially in the concrete tension zone, and then throughout the length in all deck panels. Upon further increase of load, the flexural crack width and depth increased, shear cracks initiated, and eventually intersected with the flexural cracks. Debonding of GFRP tubular sections from concrete was observed after failure in all deck panels. The deck panels started load shedding immediately after the failure load was reached and collapsed suddenly. The failure pattern of the deck panel CDS4 was shown in Fig. 3(b). The hybrid FRP/concrete deck panels failed by flexure-shear. The deck panels CDS1, CDS2, CDS3, and CDS4 did not return to their original shape after releasing of load. The safety factor against failure varied from 3.0 to 3.8.

### SCRIMP FRP Bridge Deck Panels

The load/deflection relations [Load Steps (2) and (3)] showed that the stiffness of the decks HC1, HC2, HC3, and HC4 remained constant during cyclic loading. Typical load/deflection curves for Load Step (3) of HC2 panel are shown in Fig. 4. Cracking sound due to debonding of the skin faces from the cell core was observed from the load of 179 kN (40,000 lb) in HC1, 157 kN (35,000 lb) in HC2, 179 kN (40,000 lb) in HC3, and 224 kN (50,000 lb) in HC4. The SCRIMP FRP deck panels started load shedding after the failure load was reached, and failed suddenly. The deck panels HC1 and HC2 failed due to web buckling nearer to quarter span from supports A and from B, respectively, followed by debonding of fiberglass fabric from the wrapped cell core. The deck panel HC3 failed due to web buckling nearer to midspan followed by the debonding of lower skin face from the wrapped cell core. A portion of fabric in the lower skin face at the loading point squeezed out and that was observed after failure. The deck panel HC4 failed due to web buckling nearer to middle support B followed by the debonding of the lower skin face from the wrapped cell core [Fig. 3(c)]. No punching at the loading point was observed in the deck panels after failure. After releasing the load, the deck panels HC1, HC2, HC3, and HC4 did not return to their original shape. The safety factor against failure varied from 6.6 to 8.2.

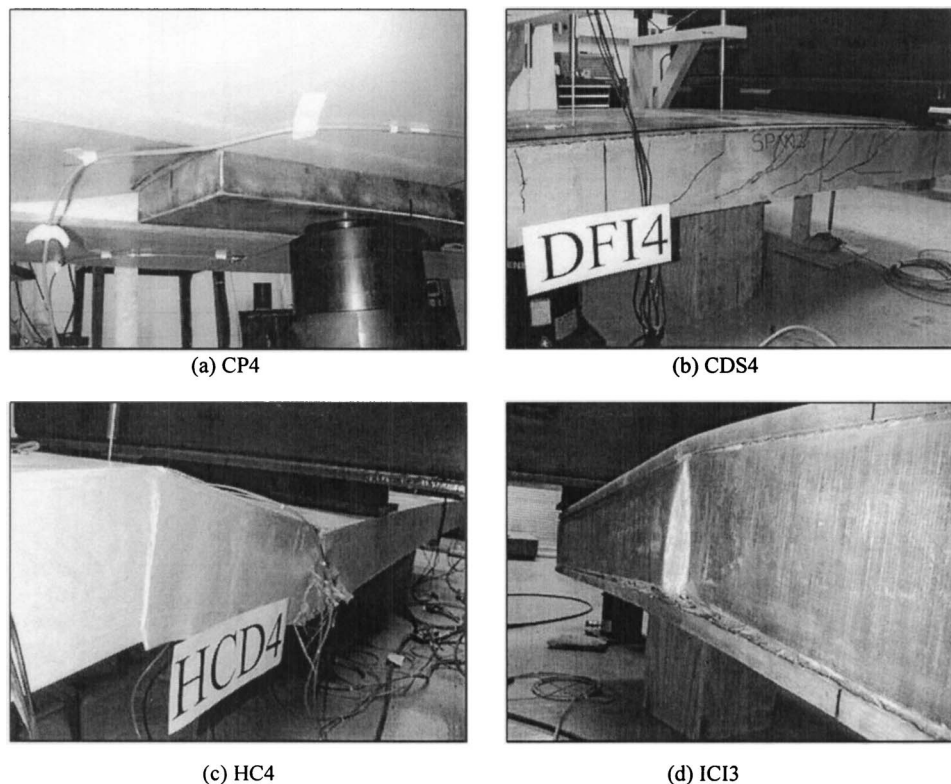
**Table 4.** Ultimate Load, Maximum Deflection, and Mode of Failure of FRP Deck Panels

Safety factor specimen	Ultimate load			Maximum deflection at ultimate load <sup>b</sup>		Mode of failure	Safety factor
	Measured (kN)	RC decks (kN)	Required <sup>a</sup> (kN)	Measured (mm)	RC decks (mm)		
CP1	664.4	191.3	528.5	39.1	29.8	Debonding-punching	5.7
CP2	659.0	199.3	534.0	61.2	33.4	Debonding-punching	5.7
CP3	651.6	183.0	539.8	98.6	41.6	Debonding-punching	5.6
CP4 Span 1	664.9	245.2	531.4	35.4	29.2	Debonding-punching	5.7
CP4 Span 2	664.9	245.2	531.4	35.3	21.9	Debonding-punching	5.7
CDS1	405.2	191.3	275.4	19.6	29.8	Flexure-shear	3.5
CDS2	438.7	199.3	284.2	22.8	33.4	Flexure-shear	3.8
CDS3	351.1	183.0	291.8	39.0	41.6	Flexure-shear	3.0
CDS4 Span 1	377.7	245.2	278.2	25.2	29.2	Flexure-shear	3.3
CDS4 Span 2	377.7	245.2	278.2	25.4	21.9	Flexure-shear	3.3
HC1	892.4	191.3	528.5	66.0	29.8	Web buckling and debonding	7.7
HC2	825.6	199.3	534.6	74.1	33.4	Web buckling and debonding	7.1
HC3	767.9	183.0	540.8	99.0	41.6	Web buckling and debonding	6.6
HC4 Span 1	953.4	245.2	531.0	50.2	29.2	Web buckling and debonding	8.2
HC4 Span 2	953.4	245.2	531.0	51.7	21.9	Web buckling and debonding	8.2
ICI1	598.0	191.3	529.7	26.6	29.8	Debonding	5.2
ICI2	724.8	199.3	537.0	49.3	33.4	Debonding	6.2
ICI3	839.9	183.0	543.5	76.4	41.6	Web buckling and debonding	7.2
ICI4 Span 1	487.1	245.2	532.4	17.6	29.2	Debonding	4.2
ICI4 Span 2	487.1	245.2	532.4	17.5	21.9	Debonding	4.2

<sup>a</sup>Required ultimate load= $1.3[1.67(LL+IL)+(DL)]$  for CDS panels and required ultimate load= $2 \times 1.3[1.67(LL+IL)+(DL)]$  for CP, HC, and ICI panels.

<sup>b</sup>The measured and baseline maximum deflections do not occur under the same load.

Note: Refer to Columns 2 and 3 of this table for the magnitude of load at failure; and safety factor=ultimate load (failure load)/factored load [1 in.=25.4 mm (1 kip=4.4482 kN)].

**Fig. 3.** Failure patterns of FRP deck panels: (a) CP4; (b) CDS4; (c) HC4; (d) ICI3

**Table 5.** Flexural and Shear Rigidities of Single Span FRP Bridge Deck Panels

Specimen	Single span panels						
	Effective span = 2,438 mm			Effective span = 3,048 mm			
	Flexural rigidity		Shear rigidity	Flexural rigidity		Shear rigidity	
$EI^a$ [N m <sup>2</sup> ( $\times 10^6$ )]	$EI^b$ [N m <sup>2</sup> ( $\times 10^6$ )]	$EI^c$ [N m <sup>2</sup> ( $\times 10^6$ )]	$GA_w^d$ [N ( $\times 10^6$ )]	$EI^a$ [N m <sup>2</sup> ( $\times 10^6$ )]	$EI^b$ [N m <sup>2</sup> ( $\times 10^6$ )]	$GA_w^d$ [N ( $\times 10^6$ )]	
CP	7.611	9.367	6.589	98.927	10.036	9.884	34.384
CDS	16.151	14.521	15.675	—	26.640	19.957	296.961
HC	5.613	6.288	4.784	65.299	8.480	9.278	46.038
ICI	9.404	9.656	6.962	54.090	10.681	11.903	123.749

<sup>a</sup>Flexural rigidity by considering shear deformation.

<sup>b</sup>Flexural rigidity from moment-curvature relationships.

<sup>c</sup>Flexural rigidity without considering shear deformation.

<sup>d</sup>The  $GA_w$  value derived from substituting the experimental data into analytical equations [1 lb = 4.4482 N (1 lb in.<sup>2</sup> = 0.00287 N m<sup>2</sup>)].

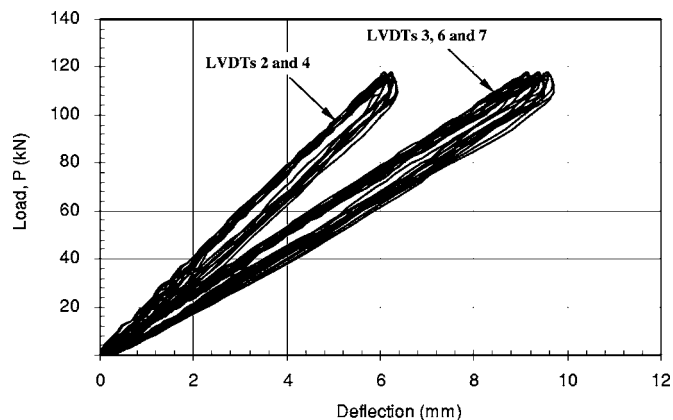


**Fig. 4.** Load versus deflection for 116 kN cyclic loading of deck panel HC2

### Contact Molding Hand Layup FRP Bridge Deck Panels

The load/deflection relations [Load Steps (2) and (3)] showed that the stiffness of the decks ICI1, ICI2, ICI3, and ICI4 remained constant during cyclic loading. Cracking sound due to debonding of the skin faces from core was heard at a load of 179 kN (40,000 lb) in ICI1, 179 kN (40,000 lb) in ICI2, 224 kN (50,000 lb) in ICI3, and 282 kN (63,000 lb) in ICI4. The contact molding hand layup FRP deck panels failed abruptly, and started load shedding immediately after the failure load was reached. The deck panels ICI1 and ICI2 failed by debonding of skin face from the cell core on the compression side. The deck panel ICI3 failed due to web buckling and debonding of top and bottom skin faces from the cell core [Fig. 3(d)]. The deck panel ICI4 failed due to debonding of skin faces close to the middle support B. Upon releasing of load the deck panels ICI1, ICI2, and ICI4 returned to its original shape and looked like the original untested specimen, however, the deck panel ICI3 did not return to its original shape. The safety factor against failure varied from 4.2 to 7.2.

### Summary and Conclusions

Tests were conducted up to failure on 16 FRP deck panels supplied by the following manufacturers: CP, CDS, HC, and ICI. Four additional RC deck panels were prepared and tested as control panels. The test panels were instrumented with LVDTs and strain gauges to measure the vertical deflections and strains, respectively. The deck panels were subjected to four loading steps in order to establish the baseline curve, to predict the response under cyclic loading, and to examine the structural behavior. The test results of FRP deck panels were compared with the performance criteria (i.e., flexure, shear, and deflection) per the ODOT, and with the test results from the RC control deck panels. The ( $EI$ ) and ( $GA_w$ ) of FRP deck panels were calculated using the first-order shear deformation beam equations, and by conducting a linear regression analysis on the load versus deflection relationship for the baseline curve. The ( $EI$ ) was also calculated using: (1) the first order beam equation without considering the shear deformation, and (2) the moment-curvature relationship on the load versus deflection relationship for the baseline curve. The factor of safety against failure of all tested FRP deck panels was calculated. The failure modes of all deck panels were reported.

**Table 6.** Flexural and Shear Rigidities of Double Span FRP Bridge Deck Panels

Specimen	Double span panels							
	Effective span=2,743 mm				Effective span=2,743 mm			
	Flexural rigidity			Shear rigidity	Flexural rigidity			Shear rigidity
	$EI^a$ [N m <sup>2</sup> (×10 <sup>6</sup> )]	$EI^b$ [N m <sup>2</sup> (×10 <sup>6</sup> )]	$EI^c$ [N m <sup>2</sup> (×10 <sup>6</sup> )]	$GA_w^d$ [N (×10 <sup>6</sup> )]	$EI^a$ [N m <sup>2</sup> (×10 <sup>6</sup> )]	$EI^b$ [N m <sup>2</sup> (×10 <sup>6</sup> )]	$EI^c$ [N m <sup>2</sup> (×10 <sup>6</sup> )]	$GA_w^d$ [N (×10 <sup>6</sup> )]
CP	30.460	11.573	4.212	11.138	18.103	12.004	3.882	11.262
CDS	16.441	8.451	7.602	32.222	15.310	9.223	7.662	34.941
HC	12.125	6.020	3.983	13.509	11.008	7.051	4.009	14.367
ICI	15.858	9.306	5.444	18.882	17.439	8.933	5.289	17.286

<sup>a</sup>Flexural rigidity by considering shear deformation.

<sup>b</sup>Flexural rigidity from moment–curvature relationships.

<sup>c</sup>Flexural rigidity without considering shear deformation.

<sup>d</sup>The  $GA_w$  value derived from substituting the experimental data into analytical equations [1 lb=4.4482 N (1 lb in.<sup>2</sup>=0.00287 N m<sup>2</sup>)].

The following conclusions are drawn based upon the static testing, and without accounting for the “knock down” factors. The double span deck panels are assumed to be representative of the panels placed on the First Salem Bridge.

1. The single and double span pultruded FRP deck–CP panels satisfy the deflection and flexure criteria.
2. The single and double span hybrid FRP/concrete deck–CDS panels satisfy the deflection and flexure criteria.
3. The single span SCRIMP FRP deck–HC panels satisfy the flexure–strain criteria but slightly exceed the deflection criteria (the ratio of measured deflection/allowable deflection varies from 1.029 to 1.059). The double span deck panel satisfies the deflection and flexure criteria.
4. The single span contact molding hand layup FRP deck–ICI panels satisfy the deflection and flexure criteria. The double span deck panel satisfies the deflection and strain limits specified in the flexure criteria but does not satisfy the required ultimate load specified in the flexure criteria [measured ultimate load=484 kN (109,000 lb), required ultimate load=528 kN (119,000 lb)].
5. All tested panels satisfied the shear criteria.
6. The safety factor against failure of the FRP bridge deck panels varied from 3 to 8.
7. The performance criteria specified by the Ohio Department of Transportation is based on strength (shear and flexure) and serviceability (deflection). The strength criteria is higher for all the FRP composite decks to account for knock down factors and the limited experience and research related to these decks. The factors of safety against failure will be different for the different deck panels since the criteria are based on an upper strength limit. Alternatively, the strength criteria can be satisfied by selecting a minimum value for the factor of safety.

The following ( $EI$ ) and ( $GA_w$ ) are recommended for use in modeling the First Salem Bridge, Ohio. These rigidities are obtained by calculating the average values of the rigidities in spans 1 and 2 for the double span panels. They are based on first-order shear deformation beam equations, and are derived by conducting a linear regression analysis on the load/deflection relationship of the baseline curve:

Pultruded FRP deck–CP panels

$$EI = 24.281 \times 10^6 \text{ N m}^2 \quad (8.461 \times 10^9 \text{ lb-in.}^2)$$

and

$$GA_w = 11.201 \times 10^6 \text{ N} \quad (2.518 \times 10^6 \text{ lb})$$

Hybrid FRP/concrete deck–CDS panels

$$EI = 15.876 \times 10^6 \text{ N m}^2 \quad (5.532 \times 10^9 \text{ lb-in.}^2)$$

and

$$GA_w = 33.584 \times 10^6 \text{ N} \quad (7.550 \times 10^6 \text{ lb})$$

SCRIMP FRP deck–HC panels

$$EI = 11.568 \times 10^6 \text{ N m}^2 \quad (4.031 \times 10^9 \text{ lb-in.}^2)$$

and

$$GA_w = 13.941 \times 10^6 \text{ N} \quad (3.134 \times 10^6 \text{ lb})$$

Contact molding hand layup FRP deck–ICI panels

$$EI = 16.651 \times 10^6 \text{ N m}^2 \quad (5.802 \times 10^9 \text{ lb-in.}^2)$$

and

$$GA_w = 18.086 \times 10^6 \text{ N} \quad (4.066 \times 10^6 \text{ lb})$$

## Acknowledgments

The writers would like to acknowledge the financial support provided by the Ohio Department of Transportation and the Federal Highway Administration and the management of the project by Professor Bahram Shahrooz at the University of Cincinnati. They also wish to acknowledge the individuals who assisted during the conduct of this research: Anthony Kordenbrock, Dr. Chelliah Madasamy, Chris Hill, Dan Eaton, David Ritchie, Everett Wilson, Joshua Johnson, Louis Mattingly, Mario Johnson, Sean Anderson, Tim Taylor, Dr. Vasudevan Krishnappa Naidu, and Dr. Vijay Gupta.

## References

- Alampalli, S., Connor, J. O., and Yannotti, A. P. (2002). "Fiber reinforced polymer composites for the superstructure of a short-span rural bridge." *Compos. Struct.*, 58(1), 21–27.
- AASHTO. (2002). *Standard specification for highway bridges*, 17th Ed., AASHTO, Washington, D.C.
- Aref, A. J., and Parsons, I. D. (2000). "Design and performance of a modular fiber reinforced plastic bridge." *Composites, Part B*, 31(6), 619–628.
- Bakht, B., Al-Bazi, G., Banthia, N., Cheung, M., Erki, M. A., Faoro, M., Machida, A., Mufti, A. A., Neale, K. W., and Tadros, G. (2000). "Canadian bridge design code provisions for fiber-reinforced structures." *J. Compos. Constr.*, 4(1), 3–15.
- Burgueno, R., Karbhari, V. M., Frieder, S., and Kolozs, R. T. (2001). "Experimental dynamic characterization of an FRP composite bridge superstructure assembly." *Compos. Struct.*, 54(4), 427–444.
- Davalos, J. F., Qiao, P., Xu, X. F., Robinson, J., and Barth, K. E. (2001). "Modeling and characterization of fiber-reinforced plastic honeycomb sandwich panels for highway bridge applications." *Compos. Struct.*, 52(3), 441–452.
- Dutta, P. K., Kwon, S. C., and Lopez-Anido, R. (2003). "Fatigue performance evaluation of FRP composite bridge deck prototypes under high and low temperatures." *Proc., 82nd Annual Meeting*, Transportation Research Board, Washington, D.C.
- Foster, D. C., Richards, D., and Bogner, B. R. (2000). "Design and installation of fiber—reinforced polymer composite bridge." *J. Compos. Constr.*, 4(1), 33–37.
- Gan, L. H., Ye, L., and Mai, Y. W. (1999). "Design and evaluation of various section profiles for pultruded deck panels." *Compos. Struct.*, 47(1), 719–725.
- Harik, I. E., et al. (1999). "Testing of concrete/FRP composite deck panels." *Proc., 5th Materials Engineering Congress on Materials and Construction*, L. C. Bank, ed., ASCE, Reston, Va., 351–358.
- Hayes, M. D., Ohanehi, D., Lesko, J. J., Cousins, T. E., and Witcher, D. (2000). "Performance of tube and plate fiberglass composite bridge deck." *J. Compos. Constr.*, 4(2), 48–55.
- Kitane, Y., Aref, A. J., and Lee, G. C. (2004). "Static and fatigue testing of hybrid fiber-reinforced polymer-concrete bridge superstructure." *J. Compos. Constr.*, 8(2), 182–190.
- Kumar, P., Chandrashekhara, K., and Nanni, A. (2004). "Structural performance of a FRP bridge deck." *Constr. Build. Mater.*, 18(1), 35–47.
- Lopez-Anido, R., and Xu, H. (2002). "Structural characterization of hybrid fiber reinforced polymer glulam panels for bridge decks." *J. Compos. Constr.*, 6(3), 194–203.
- Youn, S. G., and Chang, S. P. (1998). "Behavior of composite bridge decks subjected to static and fatigue loading." *ACI Struct. J.*, 95(3), 249–258.